Supporting Information

Role of Electronic Structure on DNA Light-Switch Behavior of Ru(II) Intercalators

Yujie Sun, Daniel A. Lutterman, Claudia Turro*
Department of Chemistry, The Ohio State University, Columbus, Ohio 43210

Synthesis and Characterization

1,10-phenanthroline-5,6-dione (dione) The ligand 1,10-phenanthroline-5,6-dione was prepared from a modification of a literature method.[S1] To a stirring solution of concentrated H_2SO_4 (140 ml) in an ice bath, 1,10-phenanthroline (10 g) was added. To this solution at 5 ºC, 17.3 g NaBr and 70 mL concentrated HNO_3 were added slowly. The mixture was stirred at room temperature for 20 min, and was then refluxed for 1 h. After it was allowed to cool to room temperature, 600 g crashed ice was added and the solution was neutralized with 30% (v/v) NaOH, then filtered. The precipitate was dissolved in 90 ºC water and filtered when hot, followed by extraction with 200 mL $CHCl_3$ three times. The organic phase was collected and after the removal of the solvent, the yellow solid was dried under vacuum. Yield: 8.1 g (76%). ^{1}H NMR (250 MHz, *CDCl$_3$*) δ(ppm): 9.13 (td, J = 4.70, 2.51, 2.51 Hz, 2H), 8.51 (dd, J = 7.88, 1.84 Hz, 2H), 7.59 (dd, J = 7.88, 4.70 Hz, 2H).

5,6-diamine-1,10-phenanthroline (diamine) According to a reported procedure, the synthesis of 1,10-phenanthroline-5,6-diamine can be accomplished in two steps.[S2] The first step involves the synthesis of the dioxime used as the starting material for the second reaction. A mixture of 5.3 g dione, 6.1 g $NH_2OH{\cdot}HCl$ and 7.5 g $BaCO_3$ were stirred and refluxed for 17 hr in 400 mL ethanol. After filtration, the residue was treated with 500 mL 0.2 M HCl and stirred for 30 min, then filtered again. The yellow solid (dioxime) was washed with H_2O, ethanol and diethyl ether successively, and finally dried under vacuum. Yield: 1.2 g (20%). The dioxime was used a starting material for the synthesis of diamine without future purification. A mixture of 0.8 g dioxime and 0.8 g Pd-C (10%) in 200 mL ethanol were purged with N_2 and heated to reflux, to which 7 mL $N_2H_4{\cdot}H_2O$ and 30 mL ethanol were added over a period of 1 h. The solution was refluxed for 18 h and was then filtered when hot through a bed of Celite, and the pad was washed with 150 mL boiling H_2O five times. The filtrate was dried under vacuum, triturated in 60 mL H_2O and kept at 4 ºC overnight. The residue was filtered and washed with cold H_2O, then dried under vacuum. Yield: 0.5 g (71%). ^{1}H NMR (250 MHz, *DMSO*) δ(ppm): 8.85-8.71 (m, 2H), 8.48 (d, J = 8.44 Hz, 2H), 7.69-7.53 (m, 2H), 5.23 (s, 4H).

Ru(bpy)$_2$Cl$_2$ was synthesized according to a method previously reported.[S3, S4] $RuC1_3{\cdot}3H_20$ (1.59 g) and 2,2'-bipyridine (1.87 g) were stirred and refluxed in 60 mL DMF for 4 h. The solution was allowed to cool to room temperature, and then kept at 0 ºC for several hours. Filtering yielded a dark green-black product, which was recrystallized in LiCl solution (30 g / 50 mL H_2O). The solid was washed with cold water and then dried under vacuum. (1.70 g, yield = 58%). 1H NMR (400 MHz, *DMSO*) δ(ppm): 9.96 (d, J = 5.10 Hz, 1H), 8.63 (d, J = 8.08 Hz, 1H), 8.49 (d, J

= 8.11 Hz, 1H), 8.07 (t, J = 7.73, 7.73 Hz, 1H), 7.76 (t, J = 6.37, 6.37 Hz, 1H), 7.66 (t, J = 7.77, 7.77 Hz, 1H), 7.49 (d, J = 4.19 Hz, 1H), 7.11 (t, J = 6.33, 6.33 Hz, 1H).

[Ru(bpy)$_2$(dione)](PF$_6$)$_2$ was prepared by a method previously reported.[S5] Ru(bpy)$_2$C1$_2$ (0.52 g) was refluxed under N_2 with dione (0.25 g))in thoroughly deareated 50/50 ethanol/water for 3 h. The mixture was allowed to cool to room temperature, and the complex was precipitated as a red solid by the addition of saturated aqueous NH_4PF_6 solution. The precipitate was washed with water and diethyl ether, dried under vacuum (0.88 g, yield = 90%). ^{1}H NMR (400 MHz, *CD$_3$CN*) δ(ppm): 8.54 (d, J = 8.10 Hz, 6H), 8.12 (tt, J = 8.22, 8.22, 1.49, 1.49 Hz, 4H), 7.99 (d, J = 4.27 Hz, 2H), 7.86 (d, J = 5.01 Hz, 2H), 7.77 (d, J = 4.99 Hz, 2H), 7.63 (dd, J = 7.94, 5.66 Hz, 2H), 7.48-7.42 (m, 4H).

[Ru(bpy)$_3$](PF$_6$)$_2$ (**1**) was synthesized in a similar way as the reported method.[S6] $RuCl_2 \cdot 2H_2O$ and excess 2,2'-bipyridine were used as starting materials. Yield = 176 mg (93%). ^{1}H NMR (400 MHz, *CD$_3$CN*) δ ppm 8.48 (d, J = 8.16 Hz, 6H), 8.04 (dt, J = 8.08, 8.08, 1.37 Hz, 6H), 7.71 (d, J = 5.55 Hz, 6H), 7.38 (ddd, J = 7.28, 5.83, 1.12 Hz, 6H). MALDI/MS, m/z: $[Ru(bpy)_3]^+$, 569.211, $[Ru(bpy)_3$–matrix$]^+$, 723.201.

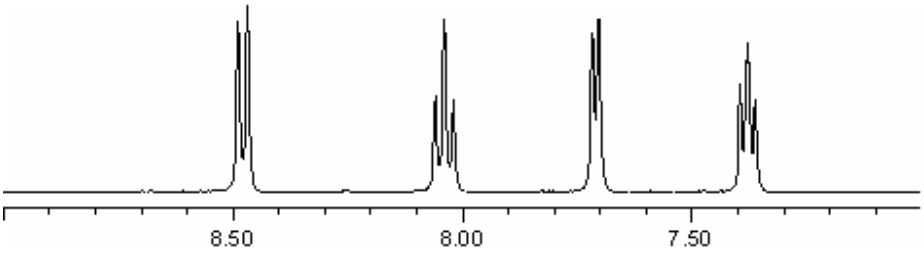

Figure S1. ^{1}H NMR of $[Ru(bpy)_3]^{2+}$ in CD_3CN.

[Ru(bpy)$_2$(tpphz)](PF$_6$)$_2$ (**2**) was synthesized by a modification of a reported method.[S7] 88.6 mg (0.42 mmol) 1,10-phenanthroline-5,6-diamine was dissolved in 45 mL hot methanol, and then poured into a boiling solution of 200 mg $[Ru(bpy)_2dione](PF_6)_2$ in 10 mL CH_3CN. The solution was refluxed at 80 ºC for 6 h, and the mixture was allowed to cool to room temperature. The resulting suspension was filtered and washed thoroughly with acetonitrile. To the concentrated filtrate in H_2O a saturated aqueous NH_4PF_6 solution was added to precipitate the product. The pure red-orange product was filtered, washed with water, ethanol, and diethyl ether and was finally dried under vacuum (185 mg, yield = 77%). ^{1}H NMR (400 MHz, *CD$_3$CN)* δ(ppm): 9.77 (d, *J* = 8.13 Hz, 2H), 9.67 (d, *J* = 8.21 Hz, 2H), 8.91 (s, 2H), 8.56 (dd, *J* = 15.78, 8.05 Hz, 4H), 8.26 (dd, *J* = 5.32, 1.27 Hz, 2H), 8.14 (dt, *J* = 8.14, 8.04, 1.46 Hz, 2H), 8.02 (dt, *J* = 8.14, 8.09, 1.45 Hz, 2H), 7.98-7.79 (m, 8H), 7.49 (ddd, *J* = 7.65, 5.61, 1.29 Hz, 2H), 7.30 (m, 2H). MALDI/MS, m/z: $[Ru(bpy)_2(tpphz)]^+$, 798.217.

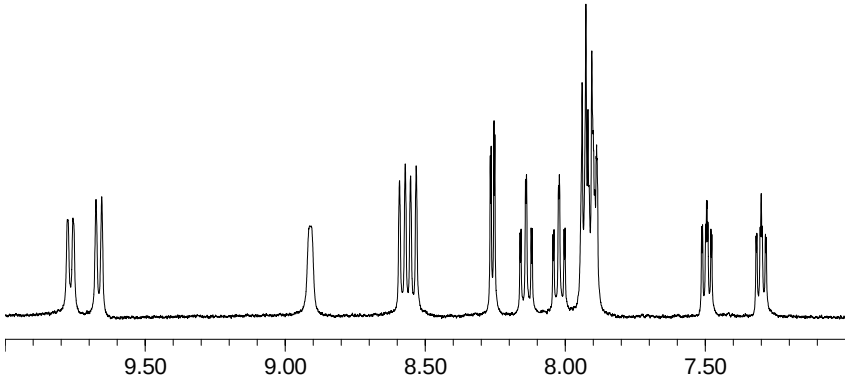

Figure S2. ^{1}H NMR of $[Ru(bpy)_2(tpphz)]^{2+}$ in CD_3CN.

$[Ru(bpy)_2(dppx)](PF_6)_2$ (**3**) was synthesized in a similar way as that for $[Ru(bpy)_2(tpphz)]^{2+}$. 100 mg $[Ru(bpy)_2(dione)]^{2+}$ (100 mg) and 4,5-dimethylbenzene-1,2-diamine (28 mg) were used as starting materials. (88 mg, yield = 79%). ^{1}H NMR (400 MHz, *CD_3CN*) δ(ppm): 9.63 (dd, *J* = 8.24, 1.31 Hz, 2H), 8.52 (dd, *J* = 13.37, 8.15 Hz, 4H), 8.21 (s, 2H), 8.11 (ddd, *J* = 9.43, 6.75, 1.37 Hz, 4H), 8.00 (dt, *J* = 8.13, 8.12, 1.47 Hz, 2H), 7.93-7.79 (m, 4H), 7.70 (dd, *J* = 5.66, 0.68 Hz, 2H), 7.45 (ddd, *J* = 7.57, 5.64, 1.29 Hz, 2H), 7.24 (ddd, *J* = 7.51, 5.64, 1.25 Hz, 2H), 2.66 (s, 6H). MALDI/MS, m/z: $[Ru(bpy)_2(dppx)]^+$, 724.290, $[Ru(bpy)_2(dppx)\text{-matrix}]^+$, 877.261.

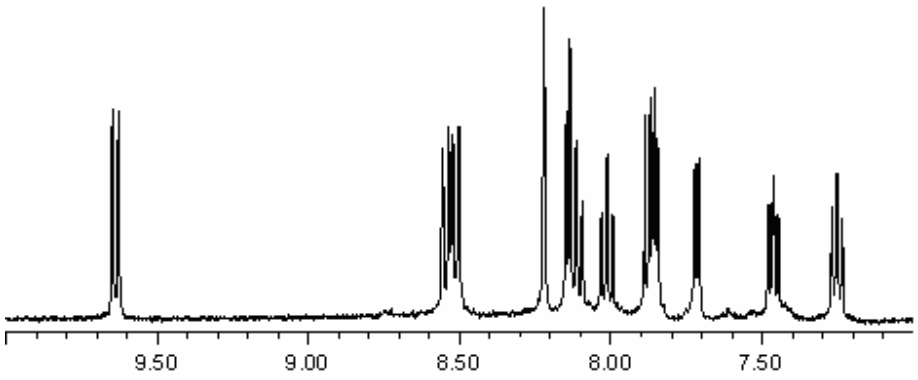

Figure S3. ^{1}H NMR of $[Ru(bpy)_2(dppx)]^{2+}$ in CD_3CN.

$[Ru(bpy)_2(dppm2)](PF_6)_2$ (**4**) was synthesized in a similar way as that for $[Ru(bpy)_2(tpphz)]^{2+}$. 100 mg $[Ru(bpy)_2(dione)]^{2+}$ (100 mg) and 3-methylbenzene-1,2-diamine (26 mg) were used as starting materials. (92 mg, yield = 84%). ^{1}H NMR (400 MHz, *CD_3CN*) δ ppm 9.74 (dd, *J* = 8.24, 1.24 Hz, 2H), 9.65 (dd, *J* = 8.24, 1.25 Hz, 2H), 8.52 (dd, *J* = 13.45, 8.14 Hz, 4H), 8.30 (d, *J* = 8.35 Hz, 2H), 8.15 (dd, *J* = 5.35, 1.18 Hz, 3H), 8.11 (dt, *J* = 7.99, 7.97, 1.40 Hz, 4H), 8.06-7.93 (m, 3H), 7.87 (ddd, *J* = 8.49, 5.54, 1.21 Hz, 4H), 7.84 (d, *J* = 5.33 Hz, 2H), 7.72 (t, *J* = 4.94, 4.94 Hz, 2H), 7.49-7.42 (m, 2H), 7.25 (m, 2H), 3.05 (s, 3H). MALDI/MS, m/z: $[Ru(bpy)_2(dppm2)]^+$, 710.335, $[Ru(bpy)_2(dppm2)\text{-matrix}]^+$, 863.238.

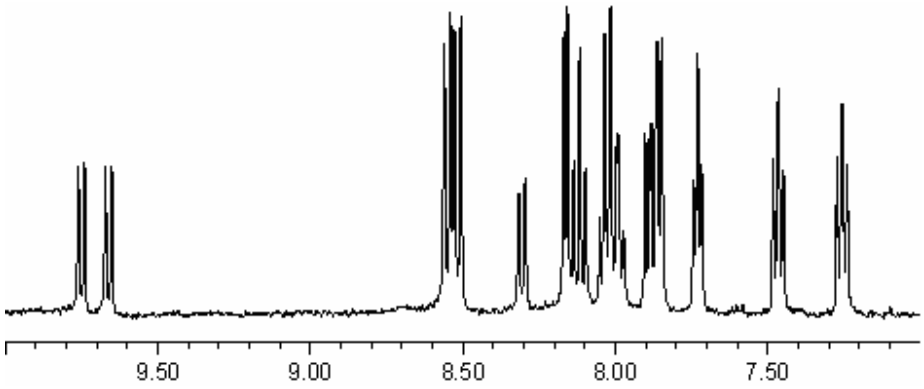

Figure S4. ^{1}H NMR of $[Ru(bpy)_2(dppm2)]^{2+}$ in CD_3CN.

$[Ru(bpy)_2(dppp2)](PF_6)_2$ (**5**) was synthesized in a similar way as that for $[Ru(bpy)_2(tpphz)]^{2+}$. $[Ru(bpy)_2(dione)]^{2+}$ (100 mg) and pyridine-2,3-diamine (23 mg) were used as starting materials. (84 mg, yield = 78%). ^{1}H NMR (400 MHz, *CD_3CN*) δ ppm 9.71 (dd, *J* = 8.24, 1.32 Hz, 1H), 9.63 (dd, *J* = 8.23, 1.31 Hz, 1H), 9.47 (dd, *J* = 4.01, 1.92 Hz, 1H), 8.84 (dd, *J* = 8.57, 1.92 Hz, 1H), 8.53 (dd, *J* = 13.28, 8.11 Hz, 4H), 8.19 (ddd, *J* = 5.37, 2.58, 1.33 Hz, 2H), 8.11 (dt, *J* = 7.99, 7.96, 1.65 Hz, 2H), 8.08 (dd, *J* = 8.52, 3.97 Hz, 1H), 8.01 (dt, *J* = 8.05, 7.99, 1.46 Hz, 2H), 7.90 (dd, *J* = 8.24, 5.39 Hz, 2H), 7.84 (ddd, *J* = 5.65, 1.39, 0.63 Hz, 2H), 7.73 (t, *J* = 4.37, 4.37 Hz, 2H), 7.46 (t, *J* = 6.64, 6.64 Hz, 2H), 7.25 (tdd, *J* = 7.07, 5.69, 1.33, 1.33 Hz, 2H). MALDI/MS, m/z: $[Ru(bpy)_2(dppp2)]^{+}$, 697.266, $[Ru(bpy)_2(dppp2)\text{-matrix}]^{+}$, 850.238.

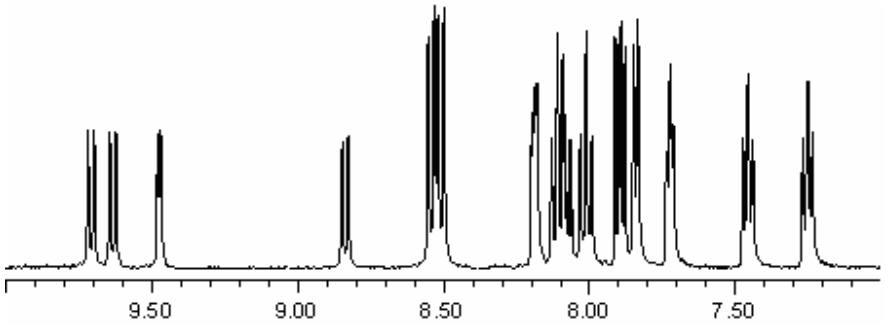

Figure S5. ^{1}H NMR of $[Ru(bpy)_2(dppp2)]^{2+}$ in CD_3CN.

$[Ru(bpy)_2(dppz)](PF_6)_2$ (**6**) was synthesized in a similar way as that for $[Ru(bpy)_2(tpphz)]^{2+}$. $[Ru(bpy)_2(dione)]^{2+}$ (100 mg) and benzene-1,2-diamine (23 mg) were used as starting materials. (82 mg, yield = 76%). 1H NMR (400 MHz, *CD_3CN*) δ ppm 9.68 (d, J = 1.32 Hz, 1H), 9.66 (d, J = 1.32 Hz, 1H), 8.53 (dd, J = 13.25, 8.07 Hz, 2H), 8.48 (dd, J = 6.58, 3.42 Hz, 4H), 8.18-8.14 (m, 4H), 8.12 (td, J = 8.10, 1.57, 1.57 Hz, 2H), 8.05-7.99 (m, 2H), 7.89 (dd, J = 8.23, 5.38 Hz, 2H), 7.87-7.84 (m, 2H), 7.75-7.71 (m, 2H), 7.47 (ddd, J = 7.60, 5.62, 1.31 Hz, 2H), 7.26 (ddd, J = 7.51, 5.68, 1.29 Hz, 2H).

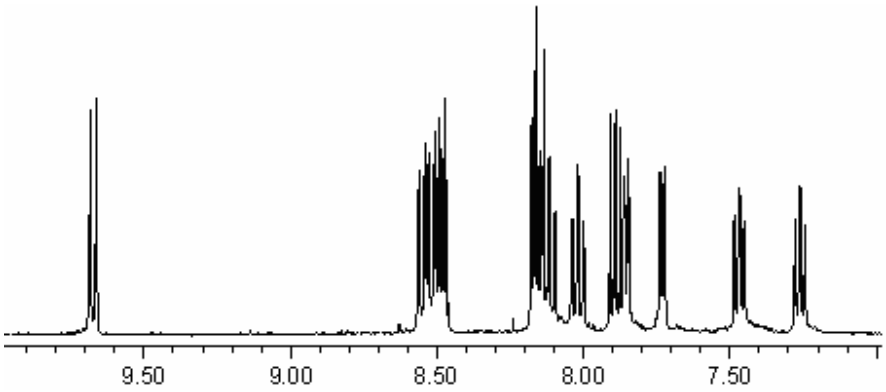

Figure S6. ^{1}H NMR of $[Ru(bpy)_2(dppz)]^{2+}$ in CD_3CN.

The chloride salts $[Ru(bpy)_2L]Cl_2$ were precipitated by addition of a saturated Bu_4NCl acetone solution to the PF_6 salt solution. The solid was filtered, washed with acetone, diethyl ether, and dried under vacuum eventually. Column purification with Saphadex G-15 was frequently employed to obtain high-purity samples when necessary for luminescence studies.

Electronic Absorption and Excitation Spectra

The electronic absorption and excitation spectra of complex **1** and **3 – 6** are overlaid in Figures S7 – S11, respectively.

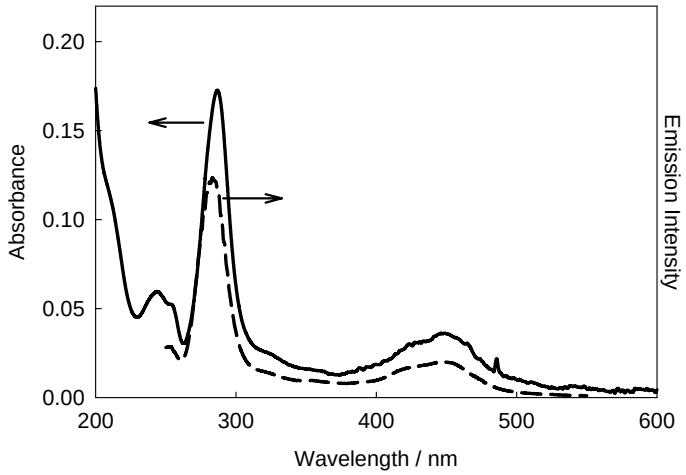

Figure S7. Electronic absorption (—) and excitation (---) spectra of **1** (1.33 μM) in CH_3CN (λ_{em} = 620 nm).

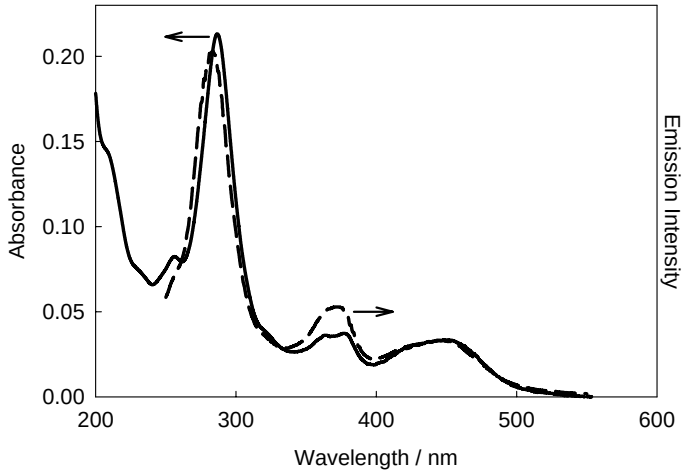

Figure S8. Electronic absorption (—) and excitation (---) spectra of **3** (1.33 μM) in CH_3CN (λ_{em} = 628 nm).

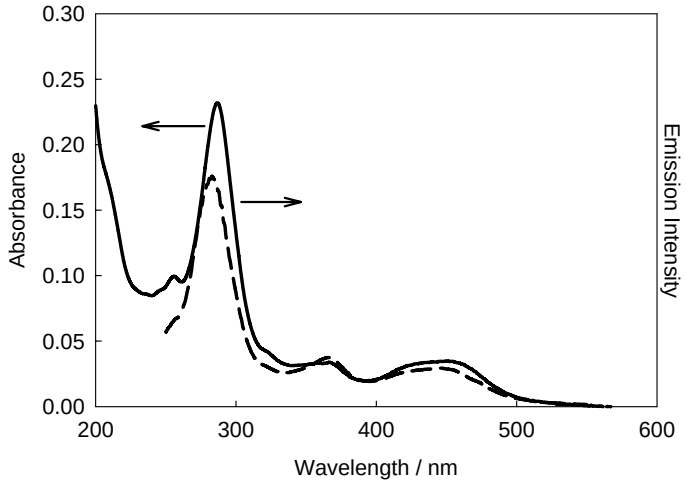

Figure S9. Electronic absorption (—) and excitation (---) spectra of **4** (1.33 μM) in CH_3CN (λ_{em} = 630 nm).

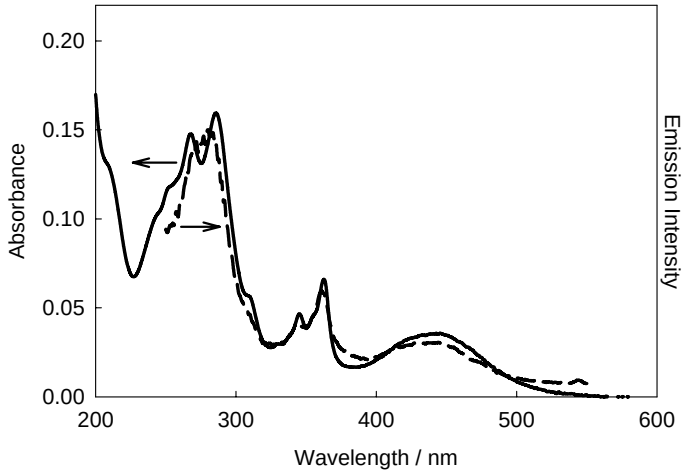

Figure S10. Electronic absorption (—) and excitation (---) spectra of **5** (1.33 μM) in CH_3CN (λ_{em} = 750 nm).

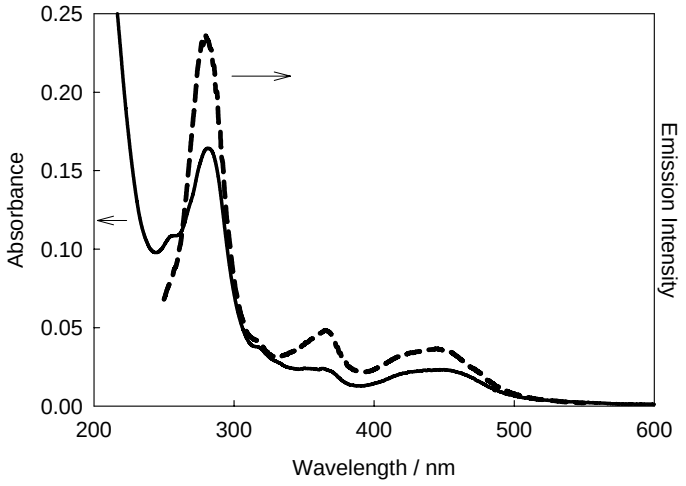

Figure S11. Electronic absorption (—) and excitation (---) spectra of **6** (1.33 μM) in CH_3CN (λ_{em} = 628 nm).

Emission Titration Plot

The DNA binding constants, K_b, of complexes **2** – **4**, were determined from fitting the changes in the emission intensity of each complex as a function of increasing DNA concentration to eq 1, which resulted in the values listed in Table 1.

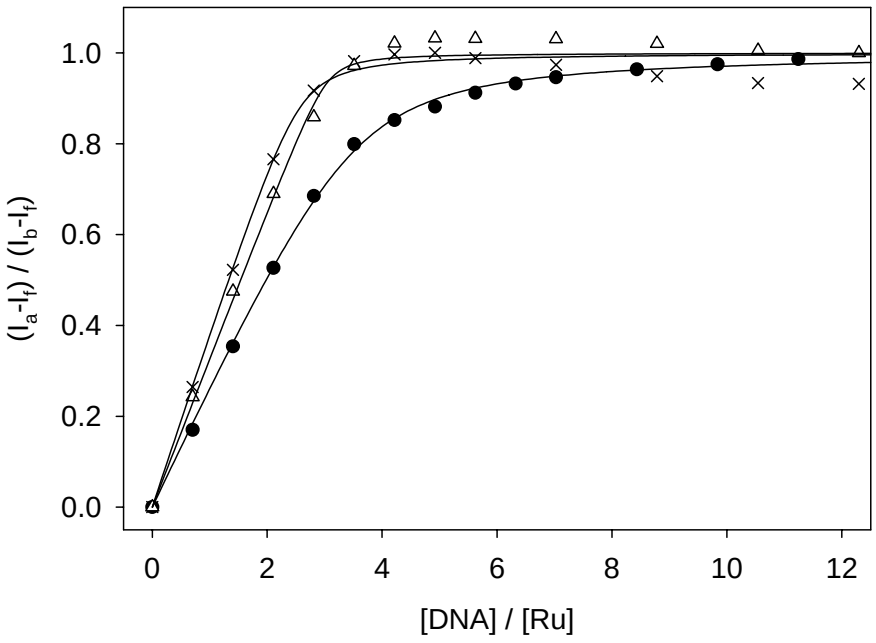

Figure S12. Plots of the luminescence titration of 10μM **2** (•), **3** (×) and **4** (Δ) with ct-DNA (5 mM Tris, pH = 7.5, 50 mM NaCl) monitored at 628 nm, 616 nm and 617 nm for **2**, **3** and **4**, respectively (λ_{ex} = 440 nm).

Electronic Structure Calculations

The electronic structure calculations of **1 - 6** were performed with density functional theory (DFT) using the Gaussian03 (G03) program package.[S8] The MOs that comprise the LUMO, LUMO+1, LUMO+2 and LUMO+3 of **1** – **6** are shown in Table S1. The energies, transition contributions, and weighting factors of calculated singlet excited states for **1** – **6** are listed in Tables S2 – S7

Table S1. Some low lying unoccupied MOs for complexes **1** – **6**. Isovalues = 0.04.

1		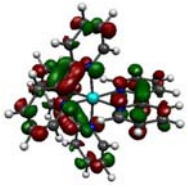 LUMO	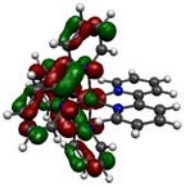 LUMO+1	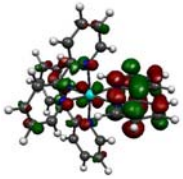 LUMO+2
2	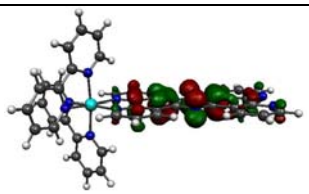 LUMO	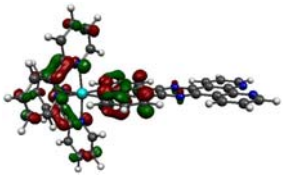 LUMO+1	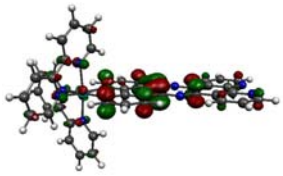 LUMO+2	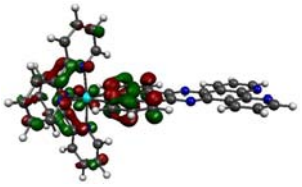 LUMO+3
3	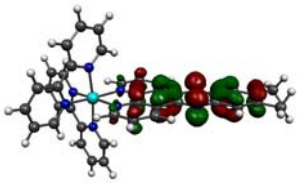 LUMO	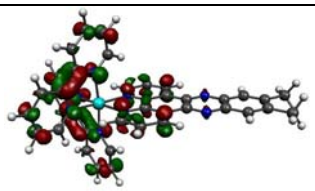 LUMO+1	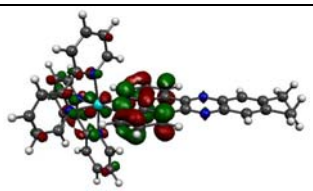 LUMO+2	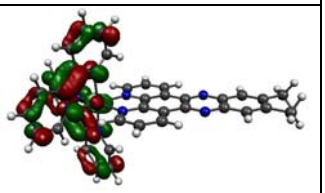 LUMO+3
4	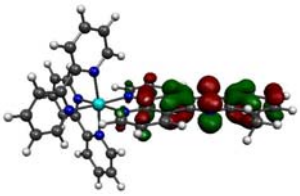 LUMO	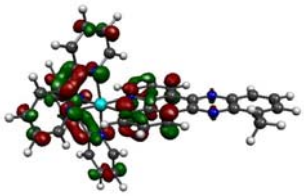 LUMO+1	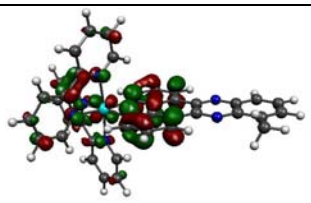 LUMO+2	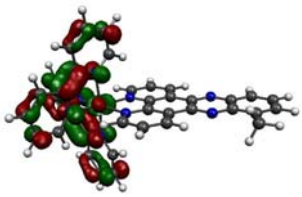 LUMO+3
5	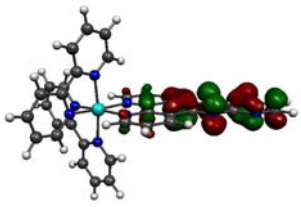 LUMO	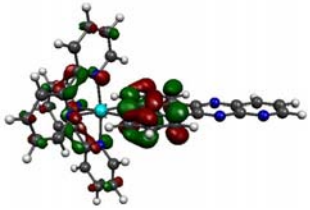 LUMO+1	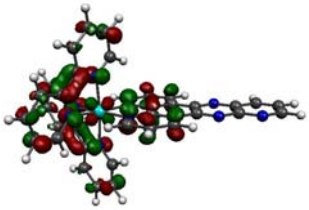 LUMO+2	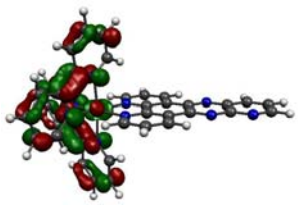 LUMO+3
6	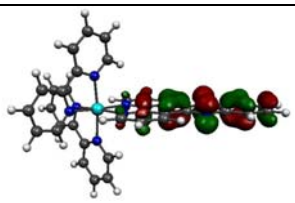 LUMO	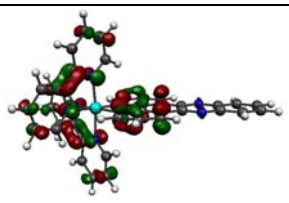 LUMO+1	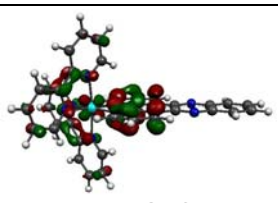 LUMO+2	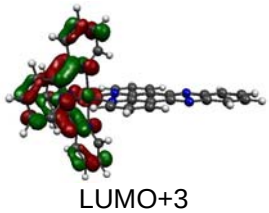 LUMO+3

Table S2. TDDFT calculations of the nine lowest energy singlet excited states of **1**, the predicted luminescence energy, and the transitions involved in each state.

Excited State	λ_{abs} / nm (f)	λ_{trip} / nm (eV)	Transition Contributions	Weighing factor
$^1ES_1$	473 (0.0017)	620 (2.00)	HOMO → LUMO	0.69574
$^1ES_2$	472 (0.0001)	620 (2.00)	HOMO → LUMO+1	0.69157
$^1ES_3$	472 (0.0001)	617 (2.01)	HOMO → LUMO+2	0.68677
$^1ES_4$	441 (0.0002)	566 (2.19)	HOMO–2 → LUMO+1 HOMO–2 → LUMO+2 HOMO–1 → LUMO+1 HOMO–1 → LUMO+2	0.13650 0.46669 0.46969 –0.13570
$^1ES_5$	437 (0.0136)	558 (2.22)	HOMO–2 → LUMO HOMO–2 → LUMO+2 HOMO–1 → LUMO HOMO–1 → LUMO+1	0.60547 0.19547 –0.18333 –0.20223
$^1ES_6$	437 (0.0143)	558 (2.22)	HOMO–2 → LUMO HOMO–2 → LUMO+1 HOMO–1 → LUMO HOMO–1 → LUMO+2	0.18232 –0.20288 0.60183 –0.20456
$^1ES_7$	419 (0.1266)	530 (2.34)	HOMO–2 → LUMO+1 HOMO–2 → LUMO+2 HOMO–1 → LUMO HOMO–1 → LUMO+1 HOMO–1 → LUMO+2	0.40646 0.17011 0.28849 –0.17092 0.40006
$^1ES_8$	419 (0.1285)	530(2.34)	HOMO–2 → LUMO HOMO–2 → LUMO+1 HOMO–2 → LUMO+2 HOMO–1 → LUMO+1 HOMO–1 → LUMO+2	–0.28137 –0.17078 0.40900 –0.40237 –0.17215
$^1ES_9$	390 (0.0000)	485 (2.56)	HOMO–2 → LUMO+1 HOMO–2 → LUMO+2 HOMO–1 → LUMO+1 HOMO–1 → LUMO+2 HOMO → LUMO+6	–0.42598 0.12543 0.12368 0.43102 0.22034

Table S3. TDDFT calculations of the six lowest energy singlet excited states of **2**, the predicted luminescence energy, and the transitions involved in each state (red = nonemissive, black = emissive).

Excited State	λ_{abs} / nm (f)	λ_{trip} / nm (eV)	Transition Contributions	Weighing factor
$^1ES_1$	486 (0.0000)	642 (1.93)	HOMO → LUMO	0.51562
			HOMO → LUMO+1	–0.33956
			HOMO → LUMO+2	–0.33308
$^1ES_2$	465 (0.0008)	608 (2.04)	HOMO → LUMO+1	–0.46353
			HOMO → LUMO+3	0.51449
$^1ES_3$	465 (0.0000)	605 (2.05)	HOMO → LUMO+2	0.40303
			HOMO → LUMO+4	0.55718
$^1ES_4$	451 (0.0026)	582 (2.13)	HOMO–2 → LUMO	0.50778
			HOMO–2 → LUMO+1	–0.31590
			HOMO–2 → LUMO+2	–0.31099
			HOMO → LUMO+1	–0.12118
			HOMO → LUMO+2	–0.10970
$^1ES_5$	449 (0.1534)	579 (2.14)	HOMO–1 → LUMO+1	0.62999
			HOMO–1 → LUMO+2	–0.28140
$^1ES_6$	447 (0.0018)	574 (2.16)	HOMO–2 → LUMO	0.13555
			HOMO → LUMO	0.46234
			HOMO → LUMO+1	0.38341
			HOMO → LUMO+2	0.30969

Table S4. TDDFT calculations of the six lowest energy singlet excited states of **3**, the predicted luminescence energy, and the transitions involved in each state (red = nonemissive, black = emissive).

Excited State	λ_{abs} / nm (f)	λ_{trip} / nm (eV)	Transition Contributions	Weighing factor
$^1ES_1$	485 (0.0000)	642 (1.93)	HOMO → LUMO	0.54590
			HOMO → LUMO+1	–0.26140
			HOMO → LUMO+3	0.35578
$^1ES_2$	467 (0.0009)	608 (2.04)	HOMO → LUMO+1	0.54503
			HOMO → LUMO+3	0.43415
$^1ES_3$	467 (0.0000)	605 (2.05)	HOMO → LUMO+2	0.69170
$^1ES_4$	450 (0.0079)	579 (2.14)	HOMO–2 → LUMO	0.52485
			HOMO–2 → LUMO+1	–0.23080
			HOMO–2 → LUMO+3	0.32884
			HOMO–1 → LUMO	0.13062
			HOMO → LUMO	0.10348
$^1ES_5$	450 (0.1185)	579 (2.14)	HOMO–2 → LUMO	0.10983
			HOMO–1 → LUMO	–0.62673
			HOMO–1 → LUMO+1	–0.25627
$^1ES_6$	445 (0.0021)	574 (2.16)	HOMO–2 → LUMO	–0.13855
			HOMO → LUMO	0.43115
			HOMO → LUMO+1	0.34181
			HOMO → LUMO+3	0.39516

Table S5. TDDFT calculations of the six lowest energy singlet excited states of **4**, the predicted luminescence energy, and the transitions involved in each state (red = nonemissive, black = emissive).

Excited State	λ_{abs} / nm (f)	λ_{trip} / nm (eV)	Transition Contributions	Weighing factor
$^1ES_1$	487 (0.0000)	642 (1.93)	HOMO → LUMO	0.55493
			HOMO → LUMO+1	–0.27849
			HOMO → LUMO+2	0.32702
$^1ES_2$	466 (0.0009)	608 (2.04)	HOMO → LUMO+1	0.51053
			HOMO → LUMO+2	0.47271
$^1ES_3$	466 (0.0000)	608 (2.04)	HOMO → LUMO+3	0.68881
$^1ES_4$	452 (0.0033)	585 (2.12)	HOMO–2 → LUMO	0.54663
			HOMO–2 → LUMO+1	–0.25595
			HOMO–2 → LUMO+3	0.30521
			HOMO → LUMO	0.10027
$^1ES_5$	452 (0.0997)	582 (2.13)	HOMO–1 → LUMO	0.64726
			HOMO–1 → LUMO+1	–0.23783
$^1ES_6$	448 (0.0022)	577 (2.15)	HOMO–2 → LUMO	–0.13767
			HOMO → LUMO	0.42153
			HOMO → LUMO+1	0.37267
			HOMO → LUMO+2	–0.37866

Table S6. TDDFT calculations of the eleven lowest energy singlet excited states of **5**, the predicted luminescence energy, and the transitions involved in each state (red = nonemissive, black = emissive).

Excited State	λ_{abs} / nm (f)	λ_{trip} / nm (eV)	Transition Contributions	Weighing factor
$^1ES_1$	517 (0.0005)	697 (1.78)	HOMO → LUMO	0.66456
			HOMO → LUMO+1	–0.18387
			HOMO → LUMO+2	0.14300
$^1ES_2$	483 (0.0497)	636 (1.95)	HOMO–1 → LUMO	0.68908
			HOMO–1 → LUMO+1	–0.11715
$^1ES_3$	478 (0.0009)	629 (1.97)	HOMO–2 → LUMO	0.67155
			HOMO–2 → LUMO+1	–0.16952
			HOMO–2 → LUMO+2	–0.12396
$^1ES_4$	466 (0.0008)	608 (2.04)	HOMO → LUMO	0.21398
			HOMO → LUMO+1	–0.29987
			HOMO → LUMO+2	–0.12396
$^1ES_5$	464 (0.0022)	605 (2.05)	HOMO → LUMO+1	0.60020
			HOMO → LUMO+2	–0.33261
			HOMO → LUMO+3	–0.10347
$^1ES_6$	464 (0.0006)	605 (2.05)	HOMO → LUMO+3	0.68236
$^1ES_7$	436 (0.0004)	557 (2.23)	HOMO–2 → LUMO	0.14995
			HOMO–2 → LUMO+1	0.18924
			HOMO–2 → LUMO+2	0.46418
			HOMO–1 → LUMO+3	–0.44871
$^1ES_8$	431 (0.0173)	550 (2.25)	HOMO–2 → LUMO+3	0.20921
			HOMO–1 → LUMO+1	0.54953
			HOMO–1 → LUMO+2	–0.37272
$^1ES_9$	431 (0.0062)	550 (2.26)	HOMO–2 → LUMO	0.14461
			HOMO–2 → LUMO+1	0.61001
			HOMO–1 → LUMO+3	0.31183
$^1ES_{10}$	416 (0.1282)	531 (2.34)	HOMO–2 → LUMO	0.38675
			HOMO–1 → LUMO+1	–0.11197
			HOMO–1 → LUMO+2	–0.36896
			HOMO–1 → LUMO+2	–0.37457
			HOMO → LUMO+2	–0.19961
$^1ES_{11}$	414 (0.1352)	522 (2.38)	HOMO–2 → LUMO+1	–0.22735
			HOMO–2 → LUMO+2	0.49378
			HOMO–1 → LUMO+3	0.41810

Table S7. TDDFT calculations of the six lowest energy singlet excited states of **6**, the predicted luminescence energy, and the transitions involved in each state (red = nonemissive, black = emissive).

Excited State	λ_{abs} / nm (f)	λ_{trip} / nm (eV)	Transition Contributions	Weighing factor
$^1ES_1$	491 (0.0001)	653 (1.90)	HOMO → LUMO	0.58242
			HOMO → LUMO+1	–0.26021
			HOMO → LUMO+2	–0.29510
$^1ES_2$	467 (0.0008)	608 (2.04)	HOMO → LUMO+1	0.49658
			HOMO → LUMO+2	–0.48893
$^1ES_3$	466 (0.0000)	608 (2.04)	HOMO → LUMO+3	0.69035
$^1ES_4$	456 (0.0875)	590 (2.10)	HOMO–1 → LUMO	0.66286
			HOMO–1 → LUMO+1	–0.20010
$^1ES_5$	455 (0.0026)	590 (2.10)	HOMO–2 → LUMO	0.56281
			HOMO–2 → LUMO+1	0.23361
			HOMO–2 → LUMO+2	0.26608
			HOMO → LUMO	0.11761
			HOMO → LUMO+1	0.14734
			HOMO → LUMO+2	0.11520
$^1ES_6$	452 (0.0019)	585 (2.12)	HOMO–2 → LUMO	0.19470
			HOMO → LUMO	0.37690
			HOMO → LUMO+1	0.39396
			HOMO → LUMO+2	0.37611

References

(S1) Zhang, Z. B.; Yan, W. P.; Fan, M. G. *Chin. J. App. Chem.* **2005,** *22*, 103.

(S2) Bodige, S.; MacDonnell, F. M. *Tetrahedron Lett.* **1997,** *38*, 8159.

(S3) Sullivan, B. P.; Salmon, D. J.; Meyer, T. J. *Inorg. Chem.* **1978,** *17*, 3334.

(S4) Giordano, P. J.; Bock, C. R.; Wrighton, M. S. *J. Am. Chem. Soc.* **1978,** *100*, 6960.

(S5) Goss, C. A.; Abruna, H. D. *Inorg. Chem.* **1985,** *24*, 4263.

(S6) Palmer, R. A.; Piper, T. S. *Inorg. Chem.* **1966,** *5*, 864.

(S7) Bolger, J.; Gourdon, A.; Ishow, E.; Launay, J. P. *Inorg. Chem.* **1996,** *35*, 2937.

(S8) Frisch, M. J. T., G. W.; Schlegel, H. B.; Scuseria, G. E.; Robb, M. A.; Cheeseman, J. R.; J. A. Montgomery, J.; Vreven, T.; Kudin, K. N.; Burant, J. C.; Millam, J. M.; Iyengar, S. S.; Tomasi, J.; Barone, V.; Mennucci, B.; Cossi, M.; Scalmani, G.; Rega, N.; Petersson, G. A.; Nakatsuji, H.; Hada, M.; Ehara, M.; Toyota, K.; Fukuda, R.; Hasegawa, J.; Ishida, M.; Nakajima, T.; Honda, Y.; Kitao, O.; Nakai, H.; Klene, M.; Li, X.; Knox, J. E.; Hratchian, H. P.; Cross, J. B.; Bakken, V.; Adamo, C.; Jaramillo, J.; Gomperts, R.; Stratmann, R. E.; Yazyev, O.; Austin, A. J.; Cammi, R.; Pomelli, C.; Ochterski, J. W.; Ayala, P. Y.; Morokuma, K.; Voth, G. A.; Salvador, P.; Dannenberg, J. J.; Zakrzewski, V. G.; Dapprich, S.; Daniels, A. D.; Strain, M. C.; Farkas, O.; Malick, D. K.; Rabuck, A. D.; Raghavachari, K.; Foresman, J. B.; Ortiz, J. V.; Cui, Q.; Baboul, A. G.; Clifford, S.; Cioslowski, J.; Stefanov, B. B.; Liu, G.; Liashenko, A.; Piskorz, P.; Komaromi, I.; Martin, R. L.; Fox, D. J.; Keith, T.; Al-Laham, M. A.; Peng, C. Y.; Nanayakkara, A.; Challacombe, M.; Gill, P. M. W.; Johnson, B.; Chen, W.; Wong, M. W.; Gonzalez, C.; Pople, J. A. **2004**.